

International Atomic Energy Agency

INDC(CCP)-220/L

---

**INDC**

**INTERNATIONAL NUCLEAR DATA COMMITTEE**

---

RADIATIVE CAPTURE CROSS SECTIONS OF  $^{236}\text{U}$  FOR  
0.15-1.1 MeV NEUTRONS

By O.T. Grudzevich, A.N. Davletshin, A.O. Tipunkov,  
S.V. Tikhonov, V.A. Tolstikov, V.V. Tuzhilov  
and L.E. Sherman

Translated by the IAEA

April 1984

---

IAEA NUCLEAR DATA SECTION, WAGRAMERSTRASSE 5, A-1400 VIENNA



RADIATIVE CAPTURE CROSS SECTIONS OF  $^{236}\text{U}$  FOR  
0.15-1.1 MeV NEUTRONS

By O.T. Grudzevich, A.N. Davletshin, A.O. Tipunkov,  
S.V. Tikhonov, V.A. Tolstikov, V.V. Tuzhilov  
and L.E. Sherman

Translated by the IAEA

April 1984

Reproduced by the IAEA in Austria  
April 1984

84-02802

## NEUTRON CONSTANTS AND PARAMETERS

UDC.539.172.4

### RADIATIVE CAPTURE CROSS-SECTIONS OF $^{236}\text{U}$ FOR 0.15-1.1 MeV NEUTRONS

O.T. Grudzevich, A.N. Davletshin, A.O. Tipunkov,  
S.V. Tikhonov, V.A. Tolstikov, V.V. Tuzhilov  
and L.E. Sherman

A high degree of accuracy, namely 3%, is required in evaluating radiative capture cross-sections of  $^{236}\text{U}$  in fast reactor calculations over the range of several kiloelectron volts to several megaelectron volts. The reason for this is the importance of  $^{236}\text{U}$  in the external fuel cycle in the accumulation chain for  $^{238}\text{Pu}$ ,  $^{236}\text{Pu}$  and  $^{232}\text{U}$  during operation of fast and hybrid reactors. For a wide neutron energy range, however, there are virtually no experimental data on capture cross-sections of  $^{236}\text{U}$ , without which it is impossible to plot the reliable recommended curve. In the 0.3-3 MeV energy range, the only available data are those from work carried out in 1961 by D. Stupegia [1] and J. Barry [2] using the activation method and these data fail to agree satisfactorily. For  $E_n < 50$  keV a paper has recently been published using the slowing-down method in lead. The results of that work stimulated the present research.

#### Measurement procedure (basic relationships)

The measurements of radiative capture cross-sections of  $^{236}\text{U}$  are carried out using the activation method with respect to the standard radiative capture cross-section of  $^{197}\text{Au}$ . These nuclides were irradiated simultaneously;  $^7\text{Li}(p,n)^7\text{Be}$  and  $\text{T}(p,n)^3\text{He}$  reactions were used as neutron sources.

Let us examine the solution of the activation equation for one of the nuclides during irradiation by an isotropic monoenergetic neutron source. In general, this solution has the form

$$C_{\varphi} \frac{\int_0^{t_0} Q(t) dt}{t_0} G \sigma_{n\gamma} N_A = \frac{\lambda N_{\gamma}}{h} F(\lambda, t), \quad (1)$$

where  $Q(t)$  is the neutron source strength in neutrons/s. (generally this is a function of time as a result of fluctuations in the proton beam current on the

accelerator target, "burn-up" of the target and other phenomena);  $G$  is a geometric factor (it is equal to the proportion of neutrons penetrating the sample from an isotropic neutron source of unit strength;  $\eta$  is the recording efficiency for induced activity;  $\sigma_{n\gamma}$  is the neutron radiative capture cross-section of the reaction;  $N_{\gamma}$  is the number of nuclei of the irradiated nuclide in the sample;  $\lambda$  is the decay constant;  $N_{\gamma}$  is the number of events, recorded by the induced activity detector;  $F(\lambda, t)$  is a time factor reducing the activity of the sample to the instant at which irradiation ceased:

$$F(\lambda, t) = \left\{ [1 - \exp(-\lambda t_0)] \exp(-\lambda t_n) [1 - \exp(-\lambda t_{\mu})] \right\}^{-1},$$

where  $t_0$ ,  $t_n$ ,  $t_{\mu}$  are the time intervals for irradiation, transfer of and variation in the induced activity;  $\phi$  is the correction for fluctuations in the neutron source strength over time. This correction factor is the ratio of the solutions of the differential equations for activation assuming that the function  $Q(t)$  remains constant over time, as does the function  $Q(t)$ , which depends arbitrarily on  $t$ :

$$C_{\varphi} = \frac{\lambda t_0 \int_0^{t_0} Q(t) \exp(-\lambda t) dt}{1 - \exp(-\lambda t_0) \int_0^{t_0} Q(t) dt}$$

Introducing in Eq. (1) the sample activity  $A$  reduced to the instant at which irradiation ceased:

$$A = \lambda N_{\gamma} F(\lambda, t) \quad (2)$$

and rewriting Eq. (1) in terms of  $\sigma$ :

$$\sigma = \frac{A}{N_{\gamma} G} \frac{1}{\eta} \frac{t_0}{C_{\varphi} \int_0^{t_0} Q(t) dt} \quad (3)$$

When irradiation of the two nuclides occurs simultaneously in the same fast neutron flux, we obtain a ratio of expressions of the Eq. (3) type for the nuclide studied ( $x$ ) and the standard nuclide ( $\ominus$ ):

$$\sigma_x / \sigma_{\ominus} = \left( \frac{A_x}{N_{\gamma x} G_x} / \frac{A_{\ominus}}{N_{\gamma \ominus} G_{\ominus}} \right) \frac{\eta_{\ominus}}{\eta_x} \frac{C_{\varphi \ominus}}{C_{\varphi x}} \quad (4)$$

For the nuclides studied the ratio  $C_{\phi_3}/C_{\phi_x}$  is close to unity with an error of less than 0.1%. Disregarding the last co-factor in Eq. (4) we obtain a formula for radiative capture cross-section of the nuclide studied:

$$\sigma_x = \sigma_3 R_\delta \eta_3 / \eta_x, \quad (5)$$

where

$$R_\delta = \left( \frac{A_x}{N_{\text{ЯX}} G_x} / \frac{A_3}{N_{\text{Я3}} G_3} \right)_\delta. \quad (6)$$

It should be noted that  $A_x$  and  $A_3$  contain corrections for activation by scattered neutrons during irradiation of the samples in the fast neutron flux and are not direct measurements. The geometric factors for the samples  $G_x$  and  $G_3$  were calculated by the Monte Carlo method, taking into account all the geometric dimensions of the target-sample system. It is assumed in the calculations that the neutron source takes the shape of a flat disc (a spot from the target beam) and that the sample is in the shape of a cylinder. The error in the calculations is about 0.2%. The numbers of nuclei in the sample  $N_{\text{ЯX}}$  and  $N_{\text{Я3}}$ , were determined from the relationship  $N_{\text{Я}} = k(N_A/A)m$ , where  $m$  is the sample mass, determined by weighing, in g;  $N_A$  is the Avogadro number;  $A_m$  is the molecular mass of the sample material;  $k$  is the number of atoms of the nuclides in a molecule of the material. The main error in determining the number of nuclei in the sample results from weighing the material on analytical scales; it can be disregarded in comparison with more significant errors in Eq. (6). Possible systematic errors due to impurities in the composition of the model do not exceed 0.15%.

#### Experimental conditions and measurement procedure

The samples in the fast neutron flux were irradiated in a KG-2.5 electrostatic accelerator. The average current at the target was about 30  $\mu\text{A}$ . The tritium targets were molybdenum discs with tritium absorbents in the form of layers of scandium and titanium. The lithium targets consisted of an LiF layer on a copper substrate.

The samples were placed in a 0.03 cm-thick cadmium container and fixed at  $0^\circ$  to the axis of the beam using a lightweight holder. The design of the target unit and irradiation assembly is shown in Fig. 1. The neutron flux was monitored

by a  $\text{BF}_3$  counter in "all-band" geometry. For each neutron energy value, four irradiations were performed, two of which were made with the weight of the target holder approximately doubled. This made it possible to measure experimentally the corrections for neutron scattering made by the design of the target holder. For some energy values we measured the contribution made by neutrons scattered by the walls of the container. In order to do this, an additional "sandwich" of samples was placed at a considerable distance from the target unit, roughly in the centre of the container. The gold samples, with a mass of about 1.15 g, consisted of discs about 0.02 cm thick and 2 cm in diameter. The manufacturers' data indicated that the impurity was about 0.01%.

The  $^{236}\text{U}$  samples were produced from  $\text{U}_3\text{O}_8$  powder by compacting 1 g of the material in a stainless steel container which was 0.01 cm thick. The internal dimensions of the container were: thickness about 0.075 cm and diameter 2 cm. The impurities did not exceed 0.15%.

The ratio of recording efficiencies for induced  $\gamma$  activity in the case of  $^{237}\text{U}$  and  $^{198}\text{Au}$  was determined separately. This ratio can be obtained by using the thermal activation cross-sections of the nuclides studied, i.e. the classical method of "two-ratios". However, poor accuracy in determining the  $^{236}\text{U}$  thermal cross-section (5.8%) leads to considerable error in the final result. Another way of determining the ratio is to make independent measurements of the detector efficiencies using absolute methods (for example the  $(4\pi\beta-\gamma)$  coincidence method). Both techniques were used in the measurements in order to double-check and exclude possible systematic errors.

The fast neutrons were irradiated in a graphite prism in the BR-1 reactor. A container with 0.1 cm-thick walls was used for the irradiation in cadmium. The choice of this thickness was based on the optimum release of epithermal components during sample activity [4].

The gold activity was recorded from the 411.8 keV  $\gamma$ -line for  $^{198}\text{Au}$ . The 208 keV line was chosen as a working line for  $^{237}\text{U}$ . Data on the decay constants of these nuclides were taken from Ref. [5]. The induced activity was measured with a gamma spectrometer containing a Ge(Li) detector with a volume of  $70\text{ cm}^3$  and a resolution for the 122 keV ( $^{57}\text{Co}$ )  $\gamma$ -line of about 2.3 keV. The spectrometer data were recorded in a "Nokia" (Finland) LP-4900 analyser. Figure 2 shows the segments of the spectra with the working lines. The peak areas  $N_\gamma$  in



the  $\gamma$ -spectra were determined with a microcomputer built into the analyser with a PROBA program, which had a similar algorithm to that described in Ref. [6].  $N_{\gamma}$  was corrected for counting errors and pulse overlap using the generator method. For samples irradiated in the accelerator, the correction did not exceed 0.5%. The time prior to measurement of the samples irradiated in the reactor was sufficiently long to reduce the correction to 0.5%.

A few remarks concerning conditions for recording the  $^{237}\text{U}$   $\gamma$ -spectrum. The background activity of the sample itself was fairly high although the most intensive low-energy part of the spectrum was quenched by the apparatus and not analysed. Where the samples were irradiated by neutrons with an energy higher than the fission threshold for  $^{236}\text{U}$  (about 0.8 MeV), the background level below the peak increased as a result of the contribution made by fragment activity to the  $\gamma$ -spectrum. After eight hours' exposure, the background level below the peak was approximately twice as high as for irradiation by neutrons with energy lower than the fission threshold. In the spectrum of the unirradiated sample in the region of the working peak there was a weak line of about 205 keV caused by a small quantity of  $^{235}\text{U}$  in the samples; its contribution to the  $^{237}\text{U}$  peak area ranged from 1-2 to 15%. The need to allow for this line tends to increase the error in determining the photopeak area for  $^{237}\text{U}$ . The absolute activity of  $^{237}\text{U}$  and  $^{198}\text{Au}$  nuclides was measured on a ( $4\pi\beta$ - $\gamma$ ) coincidence unit [7,8].

#### Ratio of recording efficiencies for the $\gamma$ -radiation detector

Let us examine the experiments conducted to determine the ratio of efficiencies of the  $\gamma$ -radiation detector.

Determination of the detector efficiency ratio by means of the ratio of thermal cross-sections. In this case the studied nuclide and standard nuclide are irradiated in the same thermal neutron flux. It is assumed in so doing that the thermal cross-sections are known. From these experiments we can make corrections for the contribution made by epithermal neutrons, self-shielding and so on. It is impossible to irradiate both nuclides together (unless the thickness of the samples is negligible), and this means that there has to be monitoring.

The authors irradiated the samples separately at the same point in the graphite prism of the BR-1 reactor. The standard and the studied nuclides were irradiated both with the cadmium containers and without them. Small additional

samples of the standard nuclide ( $^{197}\text{Au}$ ) were used as a control and placed in a fixed position relative to the basic samples, at a distance which prevented them influencing each other. The saturation activity of the irradiated sample is related to the neutron flux ( $\phi(E)$ ) by the relationship  $A = \eta N_R \int_0^\infty \sigma(E) \phi(E) dE$ .

Assuming that  $\phi(E) = W\psi(E)$ , where  $W$  is the reactor power, let us write expressions for the normalized activities of samples irradiated in the cadmium container and without it:

$$R = \frac{A/N_R}{A_M/N_{RM}} = \frac{\eta}{\eta_M} \frac{\int_0^\infty \sigma(E) \psi(E) dE}{\int_0^\infty \sigma_M(E) \psi_M(E) dE};$$

$$[R] = \frac{[A]/N_R}{A_M/N_{RM}} = \frac{\eta}{\eta_M} \frac{\int_{E_{cd}}^\infty \sigma(E) \psi(E) dE}{\int_0^\infty \sigma_M(E) \psi_M(E) dE}.$$

The subscript "m" indicates the values obtained from the control, the square brackets indicate irradiation in the cadmium container;  $E_{Cd}$  is the lower limit of the "above-cadmium" neutron spectrum. If we combine the results of the activity measurements of the studied sample and the standard sample, irradiated with and without cadmium, we obtain an expression for calculating the ratio of efficiencies:

$$\frac{\eta_3}{\eta_x} = \frac{\sigma_x^T}{\sigma_3^T} \frac{R_3 - [R_3]}{R_x - [R_x]} \frac{K_3}{K_x}. \quad (7)$$

In deriving this relationship, it is assumed that the thermal neutrons spectrum has a Maxwellian distribution and that the cross-sections in this energy region conform to the  $1/v$  law. Corrections  $K_x, K_3$  for self-shielding of the thermal neutron flux by the sample material were calculated from the equation given in Ref. [9]

$$k = \exp(\bar{\ell} \Sigma), \quad (8)$$

where  $\bar{\ell}$  is the mean path length of a neutron in the sample and  $\Sigma$  is the macroscopic activity cross-section. The mean path length in the sample in the form of a flat disc, radius  $R$  and thickness  $h$  was calculated from the equation

$$\bar{\ell} = 4V/S = \frac{2h}{1 + h/R}.$$

For the samples used,  $K_y/K_x = 1.239$  (error of 0.1%). The thermal cross-sections of the studied and standard nuclides were taken from Ref. [10]:

$\sigma_x^T(^{236}\text{U}) = 5,2 \pm 0,3 \text{ b}^* (5,8\%)$ ,  $\sigma_y^T(^{197}\text{Au}) = 98,8 \pm 0,3 \text{ b}^* (0,3\%)$ . Measurements of the second factor in Eq. (7) were  $43.50 \pm 1.5\%$ . The estimated error of each measurement was 2.1%, its components are given in Table 1. In this table and elsewhere in the text, errors are given for 68% of the confidence level.

The error in the measurement of activity includes errors in determining the area of the photopeak, errors introduced by corrections made for calculation errors and pulse overlap in the amplitude analysis tract, and also reduction of the result obtained to the moment at which irradiation ceased. These measurements are made several times for each sample in order to reduce the overall error; Table 1 gives the errors of the averaged values. We should point out that we disregarded errors in the measurement of the contribution made by epithermal neutrons since the cadmium ratios for both nuclides are relatively high. The result of this method of measuring the efficiency of the detector, taking into account the errors of all the elements in the right-hand side of Eq. (7), is  $\eta_y/\eta_x = 2.29 \pm 6\%$ .

Here are a few remarks concerning possible systematic errors:

1. The systematic error in determining the photopeak area in this method is contained in the form of ratios which should to some extent reduce its influence.

2. The packing of the  $^{236}\text{U}$  sample in the stainless steel container (0.1 mm thick) leads to excitation of the thermal neutron flux during irradiation. In order to compensate for this, the  $^{197}\text{Au}$  samples were irradiated in similar containers.

3. The calculated correction for self-shielding of the sample is valid for diffusion of the thermal neutron flux. The thermal neutron flux in the BR-1 reactor graphite prism was not identical to the isotropic flux and this may modify the mean path of the thermal neutron  $\bar{\lambda}$  in the sample by comparison with the isotropic flux. In order to evaluate the isotropy of the flux, measurements were made using  $^{197}\text{Au}$  samples irradiated both frontally to the

---

\* 1 barn =  $10^{-28} \text{ m}^2$ .

direction of the active zone and perpendicular to the direction whilst retaining the distance from the centre of the active zone to the centre of the sample. The difference obtained was approximately 2.7% which, if it is taken only in terms of the variation in  $\bar{x}$ , shows a relatively good approximation to the isotropy of the thermal neutron flux used.

4. The systematic error resulting from underestimated corrections for the depression of the thermal neutron flux and the possible deviation of the energy dependence of the cross-sections from the  $1/v$  law, was estimated approximately and may be as much as  $-(3-4)\%$ . It is being calculated more accurately.

Determination of the ratio of efficiencies of the detector by means of absolute measurements of efficiency for each nuclide. Absolute measurements of the efficiency of the  $\gamma$ -quanta detector are based on techniques by which the activity of the nuclide studied is rendered absolute. One of the most reliable techniques for measuring absolute activity is the  $(4\pi\beta-\gamma)$  method of coincidences with dual extrapolation. In these measurements, the  $(4\pi\beta-\gamma)$  coincidence method was used first to measure the absolute activity of  $^{237}\text{U}$ .

In order to determine the absolute efficiency  $\eta_3$  ( $^{198}\text{Au}$ ), it was necessary to activate the standard sample used for measuring the radiative capture cross-section and also a small sample (foil), with dimensions and mass corresponding to the requirements of the  $(4\pi\beta-\gamma)$  method of coincidences [7]. Activation of the sample and foil assembly was conducted in the centre of the BR-1 core. The "hard" neutron spectrum meant that in this case it was possible to disregard corrections for self-shielding and blocking of neutrons by the samples. After irradiation the foil disintegrates and measurements of the large sample were made using the Ge(Li) detector. The expression for its efficiency has the form:

$$\eta_3 = \frac{A}{a_0} \frac{m}{M}, \quad (9)$$

where  $a_0$  is the activity of the foil determined by the absolute method;  $m_\phi$  is the mass of the foil;  $M$  is the mass standard sample for which the efficiency of the Ge(Li) detector is determined;  $A$  is the activity of the standard sample measured by the Ge(Li) detector and reduced to the time at which the foil disintegrates:

$$A = \frac{P\lambda}{T_{\text{жс}} [1 - \exp(-\lambda t_{\text{н}})] \exp(-\lambda t_{\text{п}})},$$

where  $P$  is the area of the photopeak;  $T_x$  is the correction for calculation errors in the amplitude analysis channel;  $t_M$  is the time of measurement;  $t_n$  is the time between measurements with the detector and absolute measurements of the foil.

The efficiency obtained was  $\eta_3 = 3.05 \times 10^{-2} \pm 1.5\%$ . The error in weighing the standard sample can be ignored. The contribution made by the other components to the error are shown in Table 2.

A detailed analysis of the errors involved in rendering absolute the activity of  $^{198}\text{Au}$  by the  $(4\pi\beta-\gamma)$  coincidence method is described in Ref. [7]. The error in measuring the activity of the standard sample was based on eight measurements; the remarks made above are valid for this error. With regard to systematic errors the question remains of systematic error in determining the area of the peak. This error should be partly compensated by the fact that the result obtained is used to determine the ratios of efficiencies of the detectors.

In determining the absolute efficiency  $\eta_x$  ( $^{237}\text{U}$ ) we used the same  $(4\pi\beta-\gamma)$  coincidence method but instead of the mass ratio between the standard sample and the foil, we used the volume-mass ratio. A small amount of  $^{236}\text{U}$  (about 30 mg) was irradiated in a thermal neutron flux and dissolved in  $\text{HNO}_3$ . The foil was made by coating a gold-plated thin organic film with 0.1 ml of this solution. The standard sample of  $^{236}\text{U}$  was simulated by a  $^{238}\text{U}_3\text{O}_8$  sample depleted to  $^{235}\text{U}$ : in the  $\gamma$ -radiation spectrum for  $^{238}\text{U}$  in the region of 208 keV the peaks are not close, but the  $\gamma$ -ray absorbent properties of the materials are similar. To produce this sample we took about 20-30% more  $\text{U}_3\text{O}_8$  than was needed for producing the standard sample. The mass was recorded, the material dissolved and a known volume of the solution with  $^{237}\text{U}$  was added. It was then evaporated and  $\text{U}_3\text{O}_8$  was obtained by calcination. The amount needed to produce the standard sample was removed and packed into the standard stainless steel container. The activity of the sample obtained by this method was measured using a  $\text{Ge}(\text{Li})$  detector and the foil was rendered absolute. The formula for determining the efficiency of the detector  $\eta_x$  in this case has the form:

$$\eta_x = \frac{A}{a_0} \frac{V_\Phi}{V_{\text{одр}}} \frac{M_{\text{исх}}}{M}, \quad (10)$$

where  $V_\phi$  is the volume of the solution used to prepare the foil;  $V_{\text{odp}}$  is the volume of the solution used to prepare the model of the standard sample;  $M_{\text{icx}}$  is the initial mass of  $^{238}\text{U}_3\text{O}_8$  used to produce the standard sample.

The efficiency calculated from the experimental results was  $\eta_x = 1.40 \times 10^{-2} \pm 1.6\%$ . Errors in weighing the mass in Eq. (10) can be disregarded, the other components of the error of  $\eta_x$  are given in Table 3. Thus, the ratio of efficiencies obtained by measuring absolute efficiencies is  $\eta_\beta/\eta_x = 2.18 \pm 2.2\%$ .

The efficiency ratios  $\eta_\beta/\eta_x$  measured by the two methods, differing by about 5%, lie within the overlap limits of measurement errors. Since they were obtained in independent experiments, they have substantially different degrees of accuracy. The considerable error in determining the thermal activation cross-section of  $^{236}\text{U}$  reduces the value of the first result, although it is very useful as a means of checking the capture cross-section determined by the ratio method. Detailed analysis of the way in which the second result was obtained did not detect any possible sources of significant systematic error and the overall statistical error is considerably smaller. These facts force us to regard the efficiency ratios measured in terms of the absolute efficiencies as the final result in obtaining the radiative capture cross-section of  $^{236}\text{U}$ .

#### Correction for the background activities of the samples, induced by scattered neutrons

The aim of the experiment in which the sample is irradiated by neutrons with an average energy  $E_n$  is to determine the activity  $A_0$  of the sample, induced by the neutrons incident upon the sample directly from the source [in Eq. (2) it is referred to as A]. Since the sample is irradiated simultaneously with neutrons scattered by various components of the design, additional activity of the samples occurs which differs for the samples of different materials. The measured activity of the irradiated sample can be represented in the form  $A = A_0 + \sum_{i=1}^7 A_i$ , where  $A_i$  is the background activity induced by the neutrons from various sources. Subscript  $i$  corresponds to the following neutron sources: 1 - the walls of the compartment; 2 - the irradiated sample; 3 - the sample container; 4 - the target holder; 5 - the anisotropy of the neutron source; 6 - the sample holder; 7 - the simultaneous irradiation of the other sample. The activity  $A_0$  is calculated from the equation

$$A_0 = A - \sum_{i=1}^7 A_i. \quad (11)$$

Let us look at the procedure for calculating  $A_\gamma$ , the background correction to the sample activity, which consists of separate corrections for various background activities. A detailed method of cross-section measurement was used in our previous work. Therefore, experimental data obtained by the authors in previous work [11] has been used to calculate the background activities. The corrections are determined in the form of relative values. The symbol  $\Delta$  is used to designate corrections determined relative to experimentally measured activity  $A$  and the symbol  $\delta$  for corrections relative to the unknown activity  $A_0$ .

On the basis of the experimental data available, the majority of corrections can be calculated in the form of relative background activities:

$\Delta A_i = A_i/A$ . Using these data we can determine the correction  $A_{\delta_1} = 1 - \sum_{\substack{i=1 \\ i \neq 2}}^6 \Delta A_i$  and the activity

$$A^* = A \left( 1 - \sum_{\substack{i=1; \\ i \neq 2}}^6 \Delta A_i \right) = A_0 + A_2 + A_7. \quad (12)$$

Two corrections were determined by calculation: the correction

$$\delta A_2 = A_2/A_0 \quad (13)$$

was determined by numerical integration [12] and the correction

$$\delta A_7 = A_7/A_0 \quad (14)$$

was calculated by the Monte Carlo method [13]. Both corrections were calculated for plane-parallel neutron flux.

Using Eqs (13) and (14) we can calculate

$$A_{\gamma_2} = (1 + \delta A_2 + \delta A_7). \quad (15)$$

Using Eqs (11), (12) and (15) we obtain the background correction

$$A_{\delta} = \frac{A_{\delta_1}}{A_{\delta_2}} = \frac{1 - \sum_{\substack{i=1 \\ i \neq 2}}^6 \Delta A_i}{1 + \delta A_2 + \delta A_7}.$$

The error in  $A$  can be calculated using the usual transfer error equations for random variable functions. For  $\Delta A_i$  there are estimated errors from processing data from experiments that have already been conducted. For  $\delta A_i$  there are not yet any estimated errors; it has been assumed that errors are about 20%. The relationship between the ratio of activities  $A_x/A_y$  of the irradiated samples

for  $^{236}\text{U}$  and  $^{197}\text{Au}$  in Eq. (6) and the measurements made by the Ge(Li) spectrometer of the activities  $A(\text{U})$  and  $A(\text{Au})$  for these samples, in accordance with what we have said above, takes the form

$$\frac{A_x}{A_j} \frac{A(\text{U})A_{\gamma}(\text{U})}{A(\text{Au})A_{\gamma}(\text{Au})} = \frac{A(\text{U})}{A(\text{Au})} A_{\gamma\text{OTH}} \quad (16)$$

Table 4 gives the results of calculating  $A_{\gamma\text{OTH}}$  and some intermediate results. The meaning of the quantities in each column is clear from the headings used in the table. Values of  $A_{\gamma}$  for uranium and gold samples are shown in Fig. 3. The dependence of corrections on the energy of the neutrons in the experiments described is similar to the dependence given in Ref. [11], but the absolute values of the corrections naturally differ as a result of several differences in the quantitative design characteristics used in irradiating the samples.

Irradiation of the samples at each neutron energy value  $E_n$  was conducted with normal and heavy target holders. The correction  $A_{\gamma\text{OTH}}$  in the case of the heavy target holder was calculated in a similar way; it is 3-4% larger than that given in Table 4. A comparative analysis was conducted of experimental data obtained in Ref. [11] for correction for the target holder. As a result, an estimate of possible systematic error in  $A_{\gamma\text{OTH}}$  of 1.5% was obtained, for the whole energy range. Work is continuing to try to make the values of possible systematic error more accurate.

Results of measurements of the radiative capture cross-section of  $^{236}\text{U}$  and discussion of results

The radiative capture cross-section of  $^{236}\text{U}$  was measured for 12 neutron energy values  $E_n$ . When the energy of the neutron source  $E_n < 250$  keV the reaction was  $^7\text{Li}(p,n)^7\text{Be}$ , when  $E_n \geq 350$  keV the reaction was  $\text{T}(p,n)^3\text{He}$ .

Table 5 shows the values of  $R_B$  [cf. Eq. (5)] obtained after processing of the experimental results. These values are averages of the results obtained for the normal and the heavy target holders. The errors are obtained by quadratic summation of the errors in values in Eqs (5) and (16). The values of the standard  $^{197}\text{Au}$  radiative capture cross-section and errors in these values are given in Ref. [14]. The results for cross-sections of  $^{236}\text{U}$  calculated from Eq. (5) are given with errors obtained by the quadratic summation of the component errors. In brackets we show the radiative capture cross-sections of  $^{236}\text{U}$  without taking into account the errors in the standard cross-section.



Figure 4 shows all the available experimental data on radiative capture cross-section of  $^{236}\text{U}$ , the results of evaluations of capture cross-section and fission of  $^{236}\text{U}$  [14 and 15] and also results of theoretical calculations of capture cross-section carried out by us. In this connection, the following points should be noted. Firstly, the data of this paper are about 45% lower than the data presented in Refs [1 and 2]. Secondly, on the basis of the energy dependence of the radiative capture cross-section of  $^{236}\text{U}$  obtained theoretically, it is fair to say that our data obtained by the methods of activation and slowing-down time in lead [3] agree. Thirdly, the present experimental data agree reasonably well with the results of calculations based on the statistical theory of nuclear reactions made from the method in Ref. [16]. In these calculations the influence of fluctuations in the neutron width is effectively taken into account by introducing modified penetration coefficients from Ref. [17]. The transmission coefficients are calculated with the optical potential parameters from Ref. [18].

The initial values of the average resonance parameters  $\bar{D}_{\text{obsv}} = (15 \pm 1 \text{ eV})$  and  $\bar{\Gamma}_{\gamma\text{obsv}} = (23 \pm 1.5 \text{ MeV})$  were taken from Refs [12] and [20], respectively. It should be noted that a recent evaluation of  $\bar{D}_{\text{obsv}}$  made by Kon'shin [21] based on work in Ref. [22] gives the value  $16.2 \pm 0.8 \text{ eV}$ . The parameters of the  $^{236}\text{U}$  levels excited during non-elastic scattering are taken from tables in Ref. [23]. The density of excited levels of nuclei is determined by the normal Fermi-gas model [16]. In this case, the parameter  $a = 26.56 \text{ MeV}^{-1}$  is borrowed from Ref. [24], the "coupling" parameter is taken to be  $-0.23 \text{ MeV}$  [24].

The factor  $f(\epsilon_\gamma)$ , taking into account the fact that the radiation width increases as the excitation energy of the compound nucleus increases, takes into account the energy dependence of the photoabsorption cross-section [16]; here,  $\epsilon_{g2} = 80 A^{-1/3} \text{ MeV}$ ,  $\Gamma_g = 5 \text{ MeV}$ . The parameter moment of inertia is accepted in the rigid body approximation:  $\sigma = 0.146 A^{2/3} \sqrt{a(u-\delta)}$ . When  $\bar{D}_{\text{obsv}} = 16.5 \text{ eV}$  within the limits  $\pm 15\%$  the theory matches the experiment. Although the choice of an adequate value of  $\bar{D}_{\text{obsv}}$  for  $^{236}\text{U}$  still requires detailed experimental and theoretical study, we can say that in the case of a good description the parameter for the fitting of the theoretical curve to the experimental curve  $\bar{D}/\bar{\Gamma}_\gamma$  lies within the limits of error caused by errors in  $\bar{D}_{\text{obsv}}$  and  $\bar{\Gamma}_{\gamma\text{obsv}}$ . A description of the experimental data [1 and 2] is obtained at  $\bar{D}_{\text{obsv}}$  which is half the size of the experimental value. Here, the theoretical curve substantially differs from experimental data for  $E_n \leq 55 \text{ keV}$ .

Thus, in accordance with the theory and experimental data, in the  $E_n < 55$  keV neutron energy range these data demonstrate that the evaluations of radiative capture cross-section of  $^{236}\text{U}$  based on Refs [1 and 2] seem to be about 45% too high in the fast neutron energy range and need to be re-examined.

#### REFERENCES

- [1] STUPEGIA, D.C., HEINRICH, R.R., McCOULD, G.M., Neutron cross-section of  $^{236}\text{U}$ , Reactor Science and Technology, J. Nucl. Energy Parts A/B, 15 4 (1961) 200.
- [2] BARRY, J.F., BUNCE, J.L., PERKIN, J.L., The radiative capture cross-section of  $^{236}\text{U}$  for neutrons in the energy range 0.3-4.0 MeV, Proc. Phys. Soc. 78 503 (1961) 801.
- [3] BERGMAN, A.A., MEDVEDEV, A.N., SAMSONOV, A.E., et al., Izmerenie secheniya radiatsionnogo zakhvata nejtronov dlya  $^{236}\text{U}$  v oblasti ehnergij 0.1-50 keV (Measurement of the radiative capture cross-section of neutrons for  $^{236}\text{U}$  in the energy range 0.1-50 keV), Voprosy atomnoj nauki i tekhniki. Ser. Yadernye konstanty 45 (1982) 3-7.
- [4] MARTIN, D.N., Correction factors for Cd-covered foil measurements, Nucleonics 13 3 (1955) 52.
- [5] LORENZ, A. (Ed.) INDC (NDS) - 108/N, Proposed Recommended List of Transactinium Isotopes, Decay Data. Part 1, Half-Lives, September (1979).
- [6] PHILIPPOT, I.A., Automatic processing of diode spectrometry results, IEEE Trans. Nucl. Sci. 17 3 (1970) 446-488.
- [7] GARAPOV, Eh.F., GRYAZNOV, A.N., DAVLETSHIN, A.N., et al., "Opredelenie aktivnosti nuclida  $^{198}\text{Au}$  v fol'gakh metodom sovpadenij" (Determination of  $^{198}\text{Au}$  nuclide activity in foils by the coincidence method), Metrologiya nejtronnogo izlucheniya no reaktorakhi uskoritelyakh (Metrology of neutron irradiation in reactors and accelerators) 2nd All-Union Labour Conference, Moscow, 14-17 October 1974, T.I.M: Tsniiatom-inform (1974) 121.

- [8] GARAPOV, E.H.F., GRYAZNOV, A.N., DAVLETSHIN, A.N., et al., Metodika izmereniya aktivnosti  $^{239}\text{U}$  (Method for measuring the activity of  $^{239}\text{U}$ ), Preprint FEhI-501 Obninsk (1974).
- [9] BEKURTS, K., VIRTTS, K., Nejtronnaya fizika (Neutron Physics), Moscow, Atomizdat (1980) 250.
- [10] MUGHABGHAB, S.F., CRARBER, D.I., Neutron Cross-Sections, Resonance Parameters, BNL-325, 3rd Ed. 1 (1973).
- [11] DAVLETSHIN, A.N., TIPUNKOV, A.O., TIKHONOV, S.V., TOLSTIKOV, V.A., Fonovye popravki pri obluchenii obraztsov na ehlektrostatichestiikh uskoritelyakh (Background corrections for irradiation of samples in electrostatic accelerators), Voprosy atomnoj nauki i tekhniki, Ser. Yadernye konstanty, 3 38 (1980) 68-77.
- [12] SHORIN, V.S., Popravka na mnogokratnoe rasseyanie nejtronov v "tonkikh" obrazksakh (Correction for repeated neutron scattering in "thin" samples), Preprint FEhI-288, Obninsk (1971).
- [13] ANDROSENKO, P.A., ANDROSENKO, A.A., Vozmozhnosti kompleksa programm dlya modelirovaniya nejtronno-fizicheskikh ehksperimentov metodom Monte Carlo (Feasibility of a set of programs for simulating neutron physics experiments by the Monte Carlo method), Preprint FEhI-1300, Obninsk (1982).
- [14] ENDF/B Summary Documentation, BNL-17541 (ENDF-201), 3rd Ed., (1979).
- [15] DRAKE, M., NICHOLS, P.F., ENDF/B-V Summary Documentation, GA-8135 (1967).
- [16] BLOKHIN, A.I., IGNATYUK, A.V., PLATONOV, V.P., TOLSTIKOV, V.A., Vliyanie kollektivnykh ehffektov plotnostej urovnej na ehnergeticheskuyu zavisimost' sechenij radiatsionnogo zakhvata bystrykh nejtronov (Influence of the collective effects of level densities on energy dependence of radiative capture cross-sections of fast neutrons), Voprosy atomnoj nauki i tekhniki, Seriya Yadernye konstanty, 4 (1976) 3-14.
- [17] TEPEL, I.W., HOFMAN, N.M., WEIDENMULLER, N.A., Hauser-Feshbach formulae for medium and strong absorption, Phys. Letters 49 B (1974) 1-4.

- [18] MADLAND, D.G., YOUNG, P.G., "Nucleon-nucleus optical potential for the actinide region", Proc. Int. Conf. on Neutron Physics and Nuclear Data for Reactors and other Applied Purposes, Harwell, Sept. (1978) 349.
- [19] BENZI, V., "Neutron radiative capture cross-section calculations", Ref. [18] 288.
- [20] MOORE, M.S., "Systematic for s- and p-wave radiative capture widths for transactinium isotopes", Ref. [18] 313.
- [21] ANSHCHINOV, G.V., KON'SHIN, V.A., MASLOV, V.M., Plotnost' urovnej trans-aktinidov vblizi ehnergii svyazi nejtronov (Density of transactinide levels close to the neutron binding energy), Preprint No. 2 AN BSSR, Minsk (1982).
- [22] CARRARO, G., BRUSEGAN, A., Nucl. Phys. A 257 (1976) 333.
- [23] LEDERER, M.C., SHIRLEY, V.S., (Eds) Table of Isotopes, 7th ed. Berkeley California (1978) 1446.
- [24] DILG, W., SCUTL, W., WONACH, H., UHL, M., Level density parameters for back-shifted Fermi-gas model in the mass range  $40 < A < 200$ , Nucl. Phys. A 217 (1973) 269.

Table 1. Components of total random error  
for the second factor in Eq. (7)

Components of random error	Irradiation of the standard $^{197}\text{Au}$ sample, %		Irradiation of the studied $^{236}\text{U}$ sample, %	
	Regular	Control	Regular	Control
Activity measurement	0.97	1.11	1.01	1.0
Number of nuclei in the sample	0.03	0.3	0.1	0.3

Table 2. Components of total random error in measuring the  
efficiency of the Ge(Li) detector for  $^{198}\text{Au}$

Random error components	Error, %
Weighing of the foil	0.24
Rendering the foil absolute by the ( $4\pi\beta\text{-}\gamma$ ) coincidence method	1.44
Measurement of the activity of the standard sample	0.25

Table 3. Components of total random error in measuring the efficiency of the Ge(Li) detector for  $^{237}\text{U}$

Random error components	Error, %
Activity of the foil [( $4\pi\beta\text{-}\gamma$ ) coincidence system]	0.6
Volume of the solution used to prepare the foil	1
Activity of the sample [Ge(Li) detector]	0.4
Volume of the solution used to prepare the sample	1

Table 4. Corrections to the ratio of activities of  $^{237}\text{U}$  and  $^{198}\text{Au}$  for the influence of scattered neutrons for the normal target holder

Neutron energy, keV	Components of corrections for background activities for uranium and gold samples		Correction for background acti- vities of the samples $A_{\gamma}(\text{U})$ and $A_{\gamma}(\text{Au})$	Ratio of corrections $A_{\gamma\text{OTH}}$
	$A_{\gamma_1}(\text{U})$	$A_{\gamma_2}(\text{U})$		
	$A_{\gamma_1}(\text{Au})$	$A_{\gamma_2}(\text{Au})$		
166	$0.793^{+2.6}$	$1.024^{+0.6}$	$0.774^{+2.7}$	$1.020^{+3.9}$
	$0.800^{+2.7}$	$1.054^{+0.8}$	$0.759^{+2.8}$	
168	$0.792^{+2.6}$	$1.024^{+0.6}$	$0.773^{+2.7}$	$1.019^{+3.9}$
	$0.800^{+2.7}$	$1.054^{+0.8}$	$0.759^{+2.8}$	
174	$0.797^{+2.6}$	$1.024^{+0.6}$	$0.778^{+2.7}$	$1.023^{+3.9}$
	$0.802^{+2.7}$	$1.054^{+0.8}$	$0.761^{+2.8}$	
206	$0.802^{+2.5}$	$1.023^{+0.5}$	$0.782^{+2.7}$	$1.022^{+3.7}$
	$0.807^{+2.6}$	$1.052^{+0.7}$	$0.767^{+2.7}$	
240	$0.813^{+2.3}$	$1.023^{+0.5}$	$0.795^{+2.4}$	$1.026^{+3.5}$
	$0.811^{+2.5}$	$1.047^{+0.7}$	$0.775^{+2.6}$	
353	$0.830^{+2.1}$	$1.024^{+0.6}$	$0.810^{+2.2}$	$1.028^{+3.2}$
	$0.825^{+2.2}$	$1.046^{+0.6}$	$0.789^{+2.3}$	
459	$0.838^{+1.8}$	$1.044^{+0.9}$	$0.803^{+2.0}$	$1.020^{+3.0}$
	$0.832^{+2.0}$	$1.057^{+0.8}$	$0.787^{+2.2}$	
551	$0.853^{+1.7}$	$1.020^{+0.4}$	$0.836^{+1.8}$	$1.031^{+2.6}$
	$0.842^{+1.9}$	$1.038^{+0.5}$	$0.811^{+2.0}$	
718	$0.863^{+1.6}$	$1.017^{+0.4}$	$0.849^{+1.7}$	$1.032^{+2.5}$
	$0.852^{+1.8}$	$1.036^{+0.5}$	$0.822^{+1.9}$	
890	$0.880^{+1.6}$	$1.019^{+0.4}$	$0.864^{+1.7}$	$1.037^{+2.4}$
	$0.861^{+1.7}$	$1.034^{+0.5}$	$0.833^{+1.8}$	
1046	$0.890^{+1.5}$	$1.026^{+0.5}$	$0.877^{+1.6}$	$1.037^{+2.4}$
	$0.869^{+1.7}$	$1.039^{+0.5}$	$0.836^{+1.8}$	
1145	$0.900^{+1.5}$	$1.018^{+0.4}$	$0.884^{+1.6}$	$1.042^{+2.4}$
	$0.876^{+1.7}$	$1.033^{+0.5}$	$0.848^{+1.8}$	

Note: The errors are given as percentages.

Table 5. Results of radiative capture cross-section measurements of  $^{236}\text{U}$

Neutron energy $E_n \pm \Delta E$ , keV	Ratio of activities of $^{237}\text{U}$ and $^{198}\text{Au}$ , $R_E$	Radiative capture cross-section, mb		
		$^{197}\text{Au}$ [14]	$^{236}\text{U}$	
166 <sup>+37</sup>	0.3938 <sup>+3</sup>	253.1 <sup>+10</sup>	217.3 <sup>+10.7</sup>	(3.7)
168 <sup>+35</sup>	0.3779 <sup>+4.1</sup>	251.5 <sup>+10</sup>	207.2 <sup>+11</sup>	(4.7)
174 <sup>+29</sup>	0.3778 <sup>+4.1</sup>	247.1 <sup>+10</sup>	203.5 <sup>+11</sup>	(4.7)
206 <sup>+26</sup>	0.3756 <sup>+2.8</sup>	245.5 <sup>+5.1</sup>	201.1 <sup>+7.1</sup>	(3.6)
240 <sup>+24</sup>	0.3693 <sup>+2.7</sup>	234.4 <sup>+6.1</sup>	188.7 <sup>+7</sup>	(3.5)
353 <sup>+41</sup>	0.4368 <sup>+2.4</sup>	179.6 <sup>+6.1</sup>	171.0 <sup>+6.9</sup>	(3.3)
460 <sup>+36</sup>	0.4863 <sup>+2.3</sup>	142.7 <sup>+6.1</sup>	151.2 <sup>+6.9</sup>	(3.2)
551 <sup>+50</sup>	0.5831 <sup>+2.1</sup>	124.7 <sup>+4.1</sup>	158.5 <sup>+5.1</sup>	(3.0)
718 <sup>+45</sup>	0.8162 <sup>+2.2</sup>	99.0 <sup>+4.1</sup>	176.1 <sup>+5.1</sup>	(3.1)
891 <sup>+30</sup>	0.8715 <sup>+1.9</sup>	85.8 <sup>+4.1</sup>	163.0 <sup>+3.0</sup>	(2.9)
1046 <sup>+45</sup>	0.8453 <sup>+1.9</sup>	81.3 <sup>+7</sup>	149.8 <sup>+7.6</sup>	(2.9)
1145 <sup>+40</sup>	0.7502 <sup>+1.9</sup>	77.8 <sup>+7</sup>	127.3 <sup>+7.6</sup>	(2.9)

Note: The errors are given as percentages.



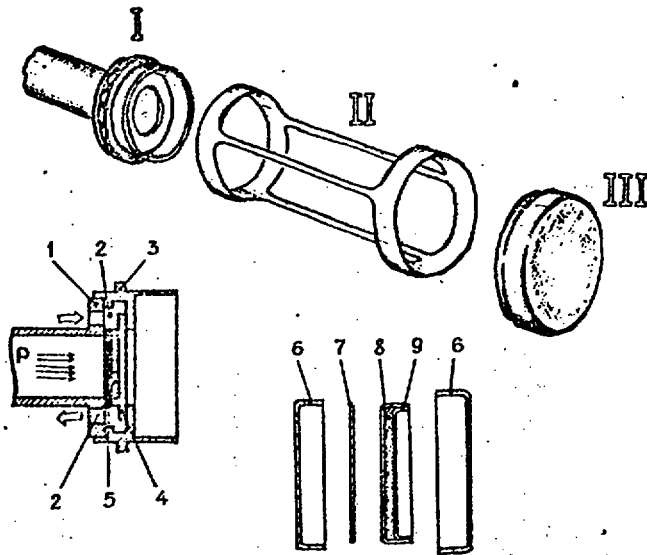


Fig. 1. Construction of the top of the target holder and sample assembly: I is the top of the target holder; II is the sample holder (about 4 cm long); III is the sample assembly in the cadmium container; 1 is the target holder; 2 is the layer of cooling water (0.35 mm thick); 3 is the cover clamp head; 4 is the cover (0.6 mm thick); 5 is the target; 6 is the cadmium container; 7 is the gold sample; 8 is the  $^{236}\text{U}$  sample (from  $\text{U}_3\text{O}_8$ ); 9 is the  $^{236}\text{U}$  sample packing container (stainless steel, 0.1 mm thick).

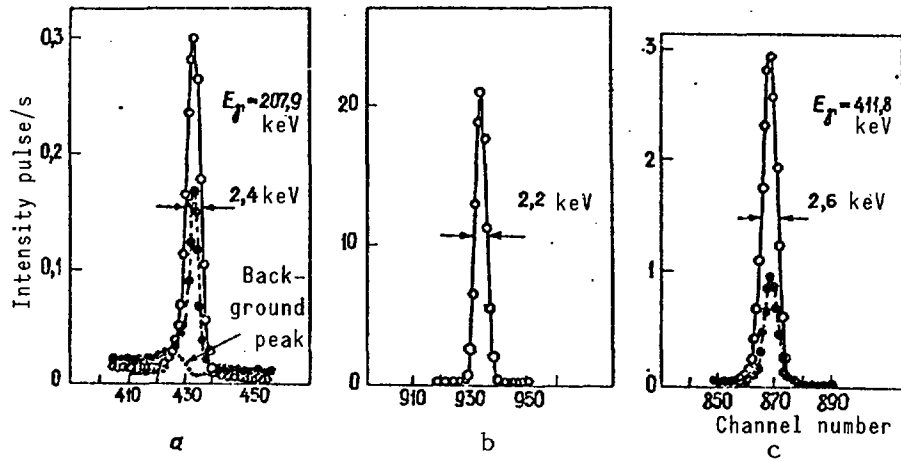


Fig. 2. Parts of the working spectra for  $^{237}\text{U}$  (a), for  $^{198}\text{Au}$  (b) and the generator peaks (c) used in correcting for counting errors and overlap (on a different scale) at neutron energy values of:  
● = 1046 keV and ○ = 166 keV.

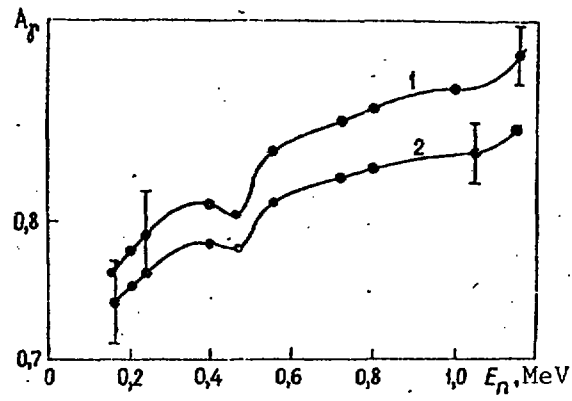


Fig. 3. Correction for neutron scattering for  $U_3O_8$  samples (curve 1) and gold (curve 2) as a function of the energy of the primary neutrons for the normal target holder.

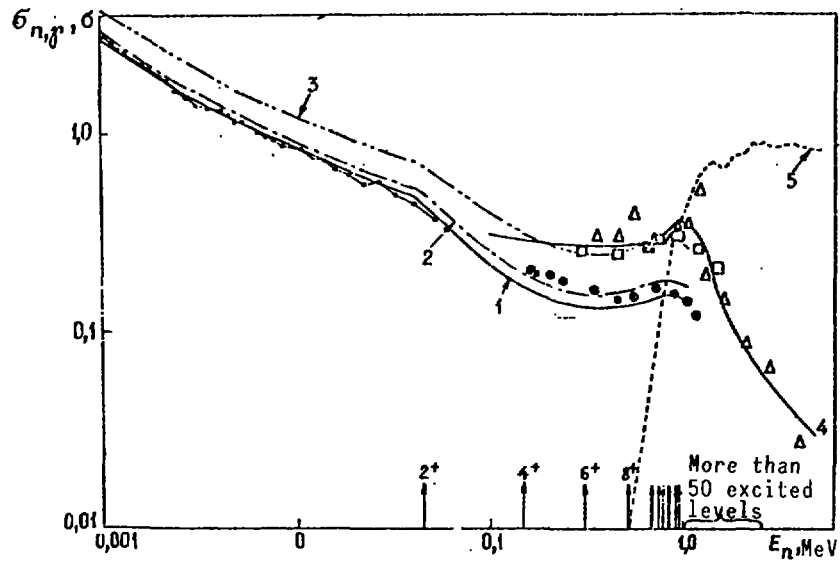


Fig. 4. Comparison of experimental data of this paper (●) with data of other authors and results of theoretical calculations:  $\Delta$  - [2, 1961];  $\square$  - [1, 1961];  $\longrightarrow$  - [3, 1982]. Curve 1 is calculated for  $D_{\text{obsv}} = 18$  eV; 2 for 15 eV; 3 for 8.7 eV. Curves 4 and 5 are the ENDF/B-V evaluations of  $^{236}\text{U}$  for  $\sigma_{n,\gamma}$  and  $\sigma_f$ , respectively, taken from Ref. [15].